JOURNAL OF MATERIALS SCIENCE 17 (1982) 2911–2918

Material-selective etching of InP and an InGaAsP alloy

F. FIEDLER, A. SCHLACHETZKI, G. KLEIN
Institut für Hochfrequenztechnik, Technische Universität Braunschweig,
D-3300 Braunschweig, West Germany

Wet chemical etchants are inexpensive and can be employed easily in device fabrication. Material-selective etchants extend the design flexibility for devices with heterostructures. Several etchants on (1 0 0) InP and LPE-grown (1 0 0) InGaAsP are studied with emphasis on smooth crystal surfaces and well-defined mesa-structures by use of photoresist. The best results are obtained with the system glycerine : HCl : $HClO_4$ for preferential attack of InP and with the system $H_2O : H_2SO_4 : H_2O_2$ for preferential etching of InGaAsP. Detailed information is given on the etching solutions investigated, on the etching conditions and the etching rates of the most useful etchants.

---

1. Introduction

In recent years the system InGaAsP/InP has become more and more important for the fabrication of optoelectronic devices such as lasers, light-emitting diodes, photodiodes, and phototransistors for fibre-communication systems. The main advantage of $In_{1-x}Ga_xAs_yP_{1-y}$ is the potential of varying the bandgap independently from the lattice constant by proper choice of the composition. For device fabrication wet chemical etching techniques are most frequently employed, because of inexpensive and easy application. Therefore many papers concerning chemical etching were published. A relatively large group of papers concentrates on etching of crystal defects. These papers are often based on the A–B etch [1] or H-etch [2] or combinations and variations thereof. Some of the more recent papers on defect etching are by Thiel and Barns [3], Kotani *et al.* [4] and Brown *et al.* [5]. This group is obviously very important for material characterization and evaluation of defects which can be detrimental to devices, such as lasers.

Another group of papers deals with etch solutions which are device-oriented. The relevant points are flat surfaces, well-defined mesa-structures, no attack of photoresist or masking films [6–8]. Only one paper is concerned with material-selective etching [9] although this is important for phototransistor fabrication [10] and will extend the flexibility in the design of integrated circuits. The situation is different in the well investigated system GaAlAs/GaAs. Here, Green [11] studied the selective etching, depending on the kind of conductivity. Tijburg and van Dongen [12] controlled the preferential etching of GaAs on GaAlAs or *vice versa* in redox systems by changing the pH value. LePore [13] varied the composition of the etching solution and along with it the pH value to effectively and selectively etch GaAs, but not GaAlAs.

Compared to GaAlAs, very little is known about InGaAsP. Phatak and Kelner [9] discuss only the preferential etching of InP on InGaAsP (not the opposite) on (1 1 1) crystallographic planes. Mostly, however, the (1 0 0) surface is used for applications. Moreover, the etched surfaces obtained are generally not smooth. Therefore, a lapping step, before the etching process, is introduced to induce work damage and thus uniform etching. To increase the etching rate, illumination is required. The etching rate mostly is not uniform, but varies with etching depth. Thus these results are of limited use for device applications.

In this paper the preferential etching of InGaAsP on InP and *vice versa* is studied on (1 0 0) crystallographic planes. A smooth etched surface is aimed at. Special emphasis is placed on mesa formation.

0022–2461/82/102911–08$03.46/0

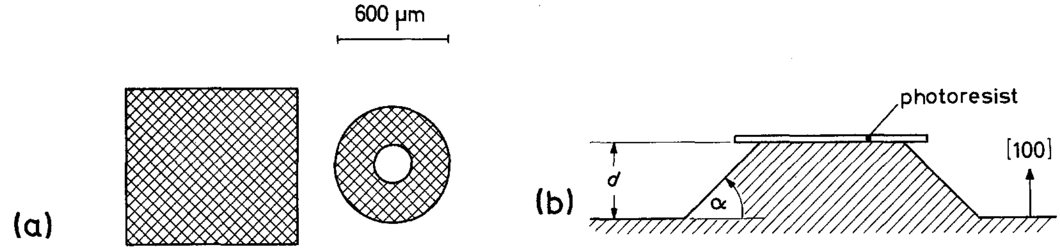

Figure 1 (a) Photolithographic pattern as defined by photoresist. (b) Definition of the quantities, which are characteristic of an etched mesa-structure. The meaning of the symbols is explained in the text.

No attack of the photoresist used for masking is of particular importance. Additionally the etching rate is determined in detail.

2. Experimental details and general considerations

For the etching experiments described here, InP bulk crystals from MCP, England, (1 0 0) oriented and mirror finished, with an etch-pits density of 2–$4 \times 10^4\,\text{cm}^{-2}$, are used. They were Sn ($n \approx 10^{18}\,\text{cm}^{-3}$) or Fe-doped ($\rho \approx 10^6\,\Omega\,\text{cm}$). Also epitaxial, unintentionally doped InP with $n \approx 10^{16}\,\text{cm}^{-3}$ was investigated. The alloy $\text{In}_{0.73}\text{Ga}_{0.27}\text{As}_{0.64}\text{P}_{0.36}$ (InGaAsP) was grown by LPE. Its bandgap as derived from absorption measurements [14] is near 1.3 μm. Triple layers of InP–buffer-layer/InGaAsP–layer/InP–cap-layer on (1 0 0) InP were employed in the final tests. The definition of etch patterns was accomplished by conventional photolithography with photoresist AZ 1350 (Shipley; Fig. 1a). Before application of the photoresist, a 15 sec etch step in 0.5% Br–isopropanol at room temperature was made, which corresponds to a removal of less than 0.1 μm according to our etching-rate measurements. To protect the samples against oxide formation, drying at 180° C under N_2 atmosphere followed. The etching was performed under magnetic stirring with about 80 rpm. A perforated teflon hose was used to bubble CO_2 or Ar along the sample which is fixed to a teflon holder by wax. The temperature of the etch solution was controlled by a thermostat (Haake F 423) to better than 1° C. The etch solutions were always freshly mixed taking care that during mixing the temperature did not rise more than 15° C above the temperature of intended use.

The etching rate was measured by a mechanical surface profiler (Perthometer C3A with pick-up unit ppk) allowing a resolution down to $0.1\,\mu\text{m}\,\text{cm}^{-1}$ in the vertical direction on the plotter. Additional cleaving and optical microscope measurements followed after the sample was etched down to less than 100 μm to facilitate cleaving.

If R_4 is the etching rate of the quaternary InGaAsP and R_2 that of the binary InP, we define a selectivity coefficient similar to [13] by:

$$S_{4/2} = \frac{R_4}{R_2} = \frac{\text{etching rate of InGaAsP}}{\text{etching rate of InP}}.$$

Non-selective etching would mean: $S_{4/2} = 1$. An example is $\text{CH}_3\text{COOH}:\text{HCl}:\text{H}_2\text{O}_2 = 2:1:1$ [7] at 55° C giving almost vertical mesa ramps in the [0 1 1] direction. Subsequently, we will describe etch solutions with a selectivity of $S_{4/2} \ll 0.02$ for preferential etching of InP, and $S_{4/2} \gtrsim 50$ for preferential etching of InGaAsP. This large difference in the preferential etch attack is achieved by different choice of the etch-solution composition. As a guideline, it can be taken that HCl does not attack GaAs, but reacts with InP [9]. Thus, InGaAsP will be resistant against HCl-based solutions. On the other hand, H_2SO_4 reacts with GaAs and thus also with InGaAsP, but only relatively mildly with InP. The other additives to the etch-solutions are required to control the etching process which is generally based on the oxidation of the samples and the subsequent dissolution of the oxidation products [15].

Frequently, etching does not result in vertical mesa ramps. Instead the ramps are inclined by an angle α with respect to the etched surface, in the present case always (1 0 0), as shown in Fig. 1b. The sloping angle α was determined either directly by microscopic inspection of the mesa-structure after removal of the photoresist, or from a microphotograph taken from a cleaved {1 1 0} plane through a mesa. Details of the mesa slope were investigated by a scanning electron microscope after deposition of a 50 nm Au film. From the depth, d, of the removed material in connection with the etching time, the etching rate was determined. Frequently, undercutting was observed as illustrated in Fig. 1b.

Undercutting as well as α usually depend on the crystallographic direction. The crystal orientation was determined by direct etching by an anisotropic etchant. Such anisotropic etch solutions can be based on HCl [7] or on H_2SO_4 [8]. They make use of the inherent symmetry properties of the zincblende structure. In this structure atoms in $\{1\,1\,1\}$ crystallographic planes are bound by three bonds in one direction normal to $\{1\,1\,1\}$ and by only one bond in the opposite direction. Consequently $\{1\,1\,1\}$ surfaces consist of only one type of atom, either In or P in the present case. This is the kind of atom which has three bonds to the crystal. Therefore, the $\{1\,1\,1\}$ planes divide into two groups, namely those consisting of group III elements, commonly called $(1\,1\,1)$A, and those consisting of group V elements called $(1\,1\,1)$B. If an In atom is the origin of the unit cell, then the $(1\,1\,1)$ plane belongs to the first group and the $(\bar{1}\,\bar{1}\,\bar{1})$ to the second one.

Neglecting details of the electronic distribution in the crystal lattice, it can be made intelligible that the two types of $\{1\,1\,1\}$ planes display marked differences in their chemical reactivity. The three electrons per In atom in the $(1\,1\,1)$A surface are all used up in establishing the bond to the crystal. Thus, $(1\,1\,1)$A is chemically very stable. Conversely, the five valence electrons per P atom in the $(1\,1\,1)$B surface are only partially saturated by the three bonds to the crystal. The two remaining electrons are available for chemical reaction, so that the $(1\,1\,1)$B is most easily attacked by chemicals. In $\{1\,0\,0\}$ planes both A and B atoms are bound by two bonds to the crystal. Neither kind will be preferred. Consequently, $\{1\,0\,0\}$ planes have medium chemical activity. Therefore, the etching rate can be expected to decrease in the order $R_{(1\,1\,1)\mathrm{B}} > R_{(1\,0\,0)} > R_{(1\,1\,1)\mathrm{A}}$ which actually was experimentally vertified [16]. As a result, it becomes clear that etch figures on $(1\,0\,0)$ InP, formed by $\{1\,1\,1\}$ or near-$\{1\,1\,1\}$ crystallographic planes, are elongated in shape in the $[0\,1\,\bar{1}]$ direction. The long walls of the etch figures are slowly etched $(1\,1\,1)$A planes or are close to them. On the opposite face of $(1\,0\,0)$ InP substrates, the elongation of etch pits is rotated by 90° [17], again because of symmetry reasons. Therefore, anisotropic etching provides an easy way of crystal orientation [7, 8, 17]. As an example, Fig. 2 shows, in its lower part, elongated etch figures of the kind discussed. In the mesa ramp leading to the unetched part of the surface, triangular etch patterns as well as the trace of the scratch on the right side of Fig. 2 are continuously elongated in the $[0\,1\,\bar{1}]$ direction with progressing etching process.

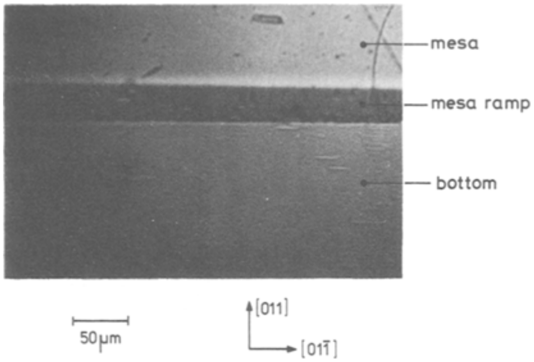

Figure 2 Etched $(1\,0\,0)$ InP surface (lower part) with elongated etch figures and triangular etch pits in the mesa ramp, as seen in a microphotograph.

Selective etch solutions like those described subsequently in detail, attack different materials differently. Therefore, they are generally reaction-rate limited rather than diffusion-limited. Consequently, a crystal-orientation dependence can be expected. A smooth crystal surface is thus the result of a compromise and not an inherent property of the etch solution.

3. Preferential etching of InP ($S_{4/2} < 1$)

3.1. The H_2O : HCl system

Concentrated HCl (37% in the present case) shows a large etching rate of about $8\,\mu\mathrm{m\,min}^{-1}$ on $(1\,0\,0)$ InP surfaces. On the other hand, InGaAsP is attacked very little. The etched surface displays thread-like structures along the $[0\,1\,1]$ direction. α was measured as 29° for mesa ramps along $[0\,1\,\bar{1}]$ and $\alpha = 36°$ for ramps along $[0\,1\,1]$ directions. For other directions, $\alpha = 90°$ can be observed. The solution $H_2O:HCl = 1:2$ has a reduced etching rate of $5\,\mu\mathrm{m\,min}^{-1}$ on $(1\,0\,0)$ planes. The etch figures are more pronounced with a surface roughness of about $0.8\,\mu$m after a $15\,\mu$m deep etching. Generally, it can be noticed that H_2O:HCl solutions are rather anisotropic particularly at increasing dilution when the character of a dislocation etchant becomes more pronounced. Therefore, this system is not useful for device fabrication.

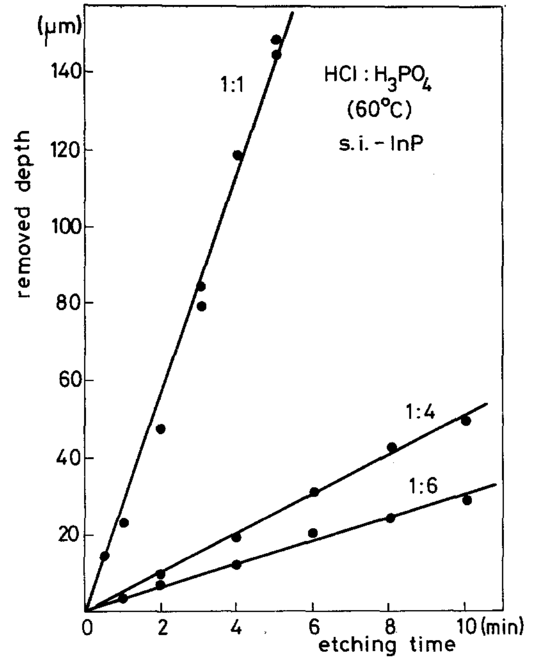

Figure 3 Etching rate of InP (1 0 0) at 60° C with the $HCl:H_3PO_4$ system for various compositions.

3.2. The HCl : H_3PO_4 system

Adding H_3PO_4 (85% H_3PO_4 in H_2O) to HCl reduces drastically the attack of InGaAsP [9]. After 30 min we noticed no change in the quaternary surface. By increasing the H_3PO_4 content the etching rate can be reduced (Fig. 3). At the same time, the appearance of etch figures is suppressed. However, the attack of photoresist increases. Further additions as $HClO_4$, glycerine or acetic acid lead to no improvements. Thus, in accordance with Phatak and Kelner [9], compositions near 1 : 1 are optimum. For this composition we determined $S_{4/2}$ as less than 10^{-3}. The mesa ramps do not ascend with uniform slope. Their main portions show an inclination angle α of 25° indicating a (3 1 1) plane for ramps parallel to $[0\bar{1}1]$ and of 35°, equivalent to $(2\bar{1}1)$, for ramps in the perpendicular direction. Fig. 4a shows an SEM photograph of a segment of the circular structure of Fig. 1a after 15 µm deep etching with the 1 : 1 composition. It can be clearly seen, that the sloping angle of the mesa-structure strongly depends on the crystallographic orientation. From the etching rate at various temperatures, as shown in Fig. 4b for the attack of $HCl:H_3PO_4 = 1:1$ on semi-insulating (s.i.) InP, an activation energy of 0.54 eV = 12.5 kcal mol^{-1} on {1 0 0} planes can be determined (Fig. 4c). We use the term "activation energy" in this paper in the sense of a parameter which conveniently describes the tem-

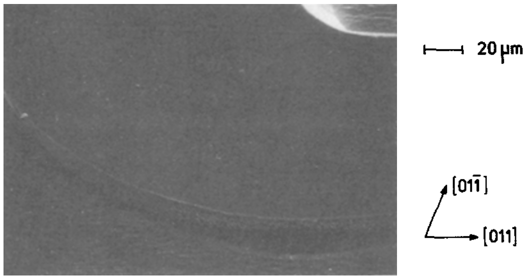

(a)

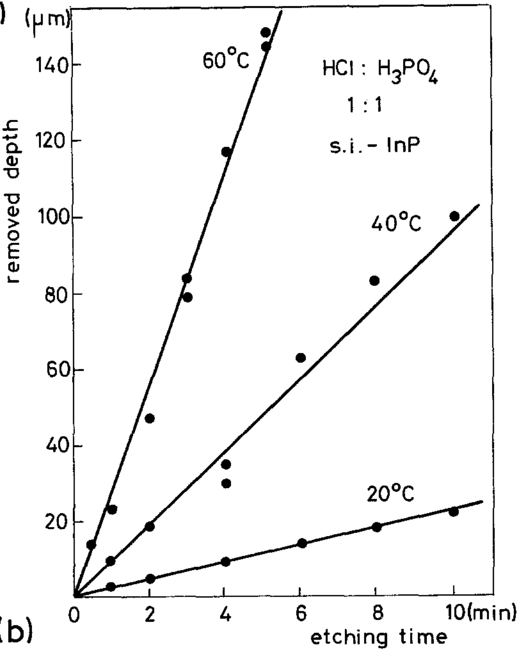

(b)

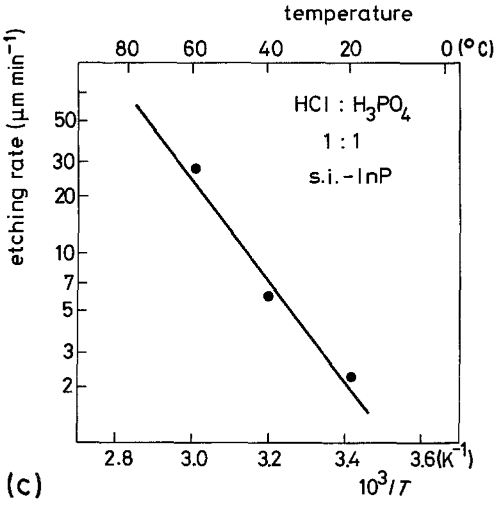

(c)

Figure 4 The $HCl:H_3PO_4 = 1:1$ etch solution: (a) SEM photograph of a segment of the circular structure (cf. Fig. 1a) after 15 µm deep etching; (b) etching rate at various temperatures; (c) etching rate dependent on reciprocal temperature.

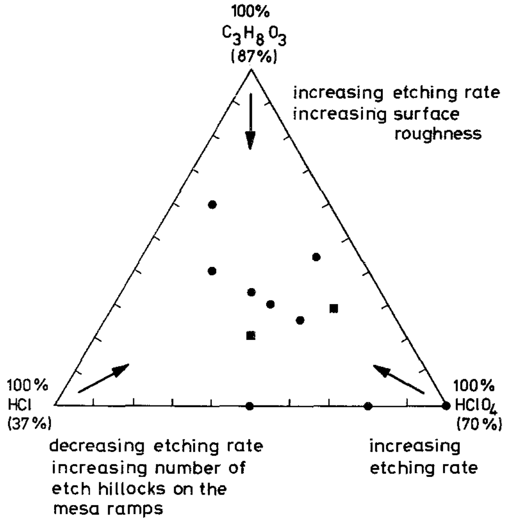

Figure 5 Etching-solution diagram of the glycerine:HCl:$HClO_4$ system; the points mark the investigated compositions. Tendencies of solution properties change in the direction of the arrows. ■ compositions described in detail in the text.

perature dependence and which can be easily used in comparing other results. A comparison of this value with the activation energies of about 0.67 eV = 15.5 kcal mol^{-1} for the (1 1 1)A planes and of 0.47 eV = 10.8 kcal mol^{-1} for the (1 1 1)B planes [9] demonstrates the different chemical reactivity of different crystallographic planes in the zinc-blende structure. These high activation energies are indicative of reaction-rate limited etching [15, 18].

3.3. The $C_3H_8O_3$: HCl: $HClO_4$ system

(Glycerine $C_3H_8O_3$, $HOCH_2CH(OH)CH_2OH$ of 87% concentration; $HClO_4$ of 70% concentration.) An improvement of the surface quality can be expected by the addition of $HClO_4$ since it does not attack InGaAsP nor InP. A composition of HCl:$HClO_4$ = 1:1 has a relatively high etching rate of about 6 μm min^{-1} and does not attack InGaAsP ($S_{4/2}$ less than 10^{-3}). Increasing the $HClO_4$ content decreases the etching rate, but at the expense of large undercutting and photoresist attack. Additions of acetic acid did not improve the results. Combination $C_3H_8O_3$:HCl:$HClO_4$ has a lower etching rate and produces relatively smooth surfaces. The influence of the components on the property of the etch solution is shown in Fig. 5. The points mark the compositions which were investigated. Two of them (squares in Fig. 5), which are the most suitable for application with $S_{4/2}$ values less than 10^{-3} will now be described in more detail, beginning with the ratio 2:1:4 by volume. The etched (1 0 0) surface is relatively smooth. For mesa ramps parallel to the $[0\bar{1}1]$ direction, $\alpha \approx 22°$, and for the ramps parallel to the [0 1 1] direction, $\alpha = 57°$. On the ramps parallel to the [0 1 1] direction many triangular etch hillocks appear, typical for near-(1 1 1)B surfaces. Scratches become visible as etch grooves similar to those in the H_2O:HCl system. The depth removed dependent on etching time is given in Fig. 6a for various temperatures. Since the dehydration of glycerine by the acid $HClO_4$ is intensified at increasing temperatures, the etching rate near 40° C is saturating. In practice the maximum temperature should be 30° C. The activation energy is 0.59 eV = 13.6 kcal mol^{-1}.

Higher etching rates must be used to produce mesa ramps of better quality. Such improved results are realized with the composition 1:2:2. The attack of InP is shown in Fig. 6b. The activation energy which is derived from Fig. 6c is 0.61 eV = 14.1 kcal mol^{-1}. Fig. 7 shows the good etching results. Smooth mesa ramps are obtained with this etch composition. Only at mesa corners were irregularities observed (Fig. 7b). The ramp parallel to the $[0\bar{1}1]$ direction has an inclination angle α of about 20° and the ramp parallel to the perpendicular direction has $\alpha \approx 30°$. As can be expected for selectively etching solutions, the etching rates for *n*-type and semi-insulating material are very similar (Fig. 6).

A number of further etching solutions, which were examined are summarily characterized in Table I.

4. Preferential etching of InGaAsP ($S_{4/2} > 1$)

The etching properties of the system H_2O:H_2SO_4:H_2O_2 with respect to InP and InGaAsP, and with respect to InP were reported by Hsieh and Shen [19] and by Nishitani and Kotani [6], respectively. Here, the solutions H_2O:H_2SO_4:H_2O_2 = 1:3:1 and 1:5:1 with H_2SO_4 95% and H_2O_2 30% were studied. Both solutions have similar properties. The results are collected in Table II. For practical use the 1:3:1 composition has been preferred, because of its lower exothermal heating during mixing of the solution.

The depth of removed LPE-grown InGaAsP, dependent on etching time is shown in Fig. 8 for different temperatures and compositions. These

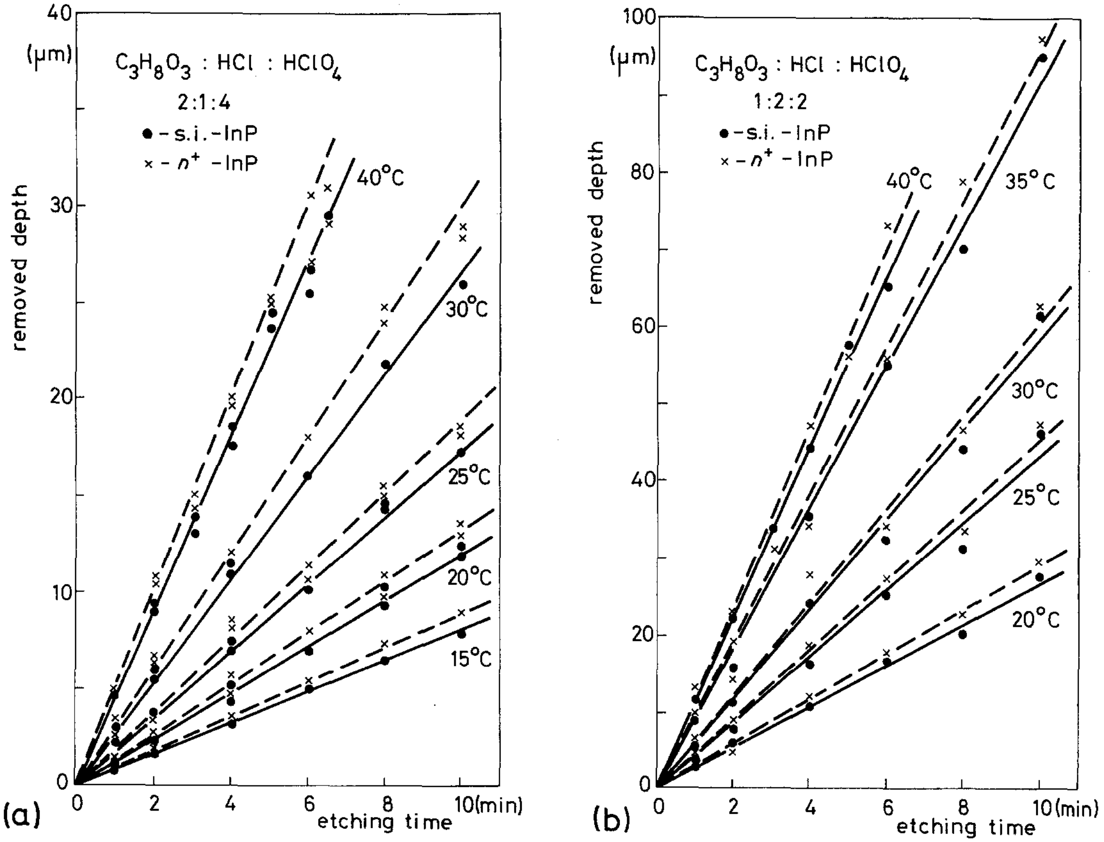

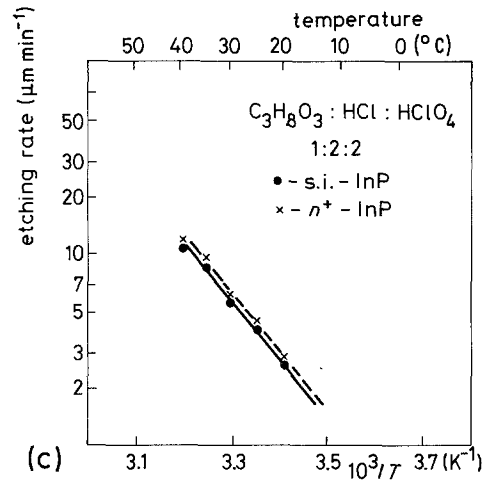

Figure 6 Dependence of removed depth on etching time (a) for glycerine:HCl:$HClO_4$ = 2:1:4 and (b) for 1:2:2 composition with the temperature as parameter. (c) Dependence of etching rate on reciprocal temperature for the etch solution of (b).

etching solutions produce smooth mesa ramps with few irregularities (compare Fig. 9b) and inclination angles between 30° and 40°. The undercutting is very low. For the composition 1:3:1, the activation energy is around 0.6 eV or 14 kcal mol^{-1}.

5. Final test

In a final test of the selective properties of the

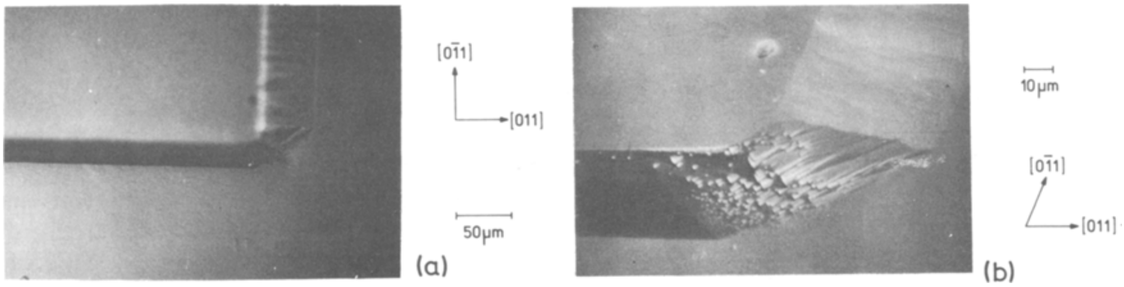

Figure 7 n-InP after etching for 5 min in glycerine:HCl:$HClO_4$ = 1:2:2; removed depth 16 µm. (a) Photograph with interference-contrast light microscope; (b) SEM photograph of the corner of the mesa from (a).

TABLE I Investigated etching solutions preferentially attacking InP and not mentioned in the text

Etching system	Composition	Characterization
$H_2O_2:H_3PO_4:HCl$	2:1:1; 1:1:1; 1:2:2	Decreasing etching rate for increasing H_2O_2 content; etch patterns on etched surface; poor mesa ramp quality
$CH_3COOH:H_2O_2:H_3PO_4:HCl$	2:1:1:1; 1:2:2:2; 4:2:1:1	Very low etching rate for large acetic acid to H_2O_2 ratio
$CH_3COOH:H_3PO_4:HCl$	2:1:1	Very rough surface
$CH_3COOH:H_3PO_4:HCl:HClO_4$	2:1:1:3	Wavy etch-pit pattern; pyramidal etch hillocks on near-{1 1 1}B mesa ramps
$CH_3COOH:HCl:HClO_4$	2:1:2; 5:1:5; 2:1:4; 2:1:10	Increasing etching rate for increasing HCl content; skin-like surfaces and glittering mesa ramps for high $HClO_4$ content
$C_2H_6O_2:CH_3COOH:HCl:HClO_4$ (ethyleneglycol)	*a*:*b*:*c*:*d*; 10 compositions with *a* from 1 to 3; *b* from 1 to 12; *c* from 1 to 6; *d* from 1 to 16	Large undercutting; mesa ramps with numerous pyramidal etch hillocks on near-{1 1 1}B mesa ramps
$C_3H_8O_3:CH_3COOH:HCl:HClO_4$ (glycerine)	*a*:*b*:*c*:*d*; 10 compositions with *a* from 2 to 14; *b* from 1 to 9; *c* from 1 to 5; *d* from 1 to 12	Relatively smooth surfaces, but large undercutting; mesa ramps relatively smooth for most compositions

TABLE II Measured results of the $H_2O:H_2SO_4:H_2O_2$ system

Volume ratio	Temperature (° C)	Etching rate (μm min^{-1}) on		$S_{4/2}$	Etching rate (μm min^{-1}) on semi-insulating InP	$S_{4/2}$
		InGaAsP	n^+ InP			
1:3:1	20	0.7	0.014	50	0.013	54
1:3:1	30	1.6	0.035	43	0.029	52
1:5:1	20	0.6	0.012	50	0.011	55
1:5:1	30	–	0.030	–	0.025	–

solutions described above, a double-mesa-structure was etched as shown in Fig. 9. The structure was delineated by use of conventional photolithographic techniques. In a first etching step the InP cap layer, 4–5.5 μm thick, was removed with $C_3H_8O_3:HCl:HClO_4 = 1:2:1$ at 20° C. Subsequently the quaternary layer with a thickness of around 3 μm was etched with $H_2O:H_2SO_4:H_2O_2 = 1:3:1$ at 20° C. In both etching steps the etching time (see Fig. 9) was chosen 20% higher than that required to remove the given layer thickness. The excellent quality of the mesa ramps, especially for the $H_2O:H_2SO_4:H_2O_2 = 1:3:1$ etching solution, is illustrated by Fig. 9b. The selectivity of the etching solutions is very good as demonstrated by the photograph of a cleaved mesa (Fig. 10).

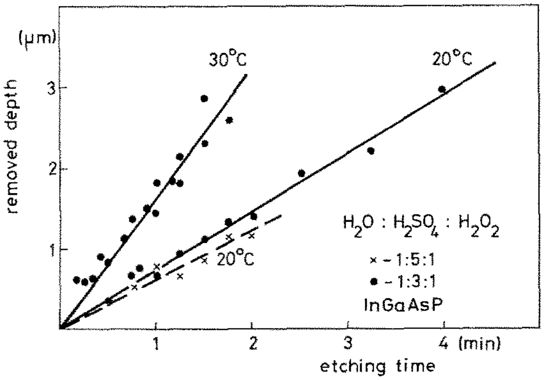

Figure 8 Etching of InGaAsP with the $H_2O:H_2SO_4:H_2O_2$ system for different temperatures and different compositions.

6. Conclusions

This paper describes a number of etchants in view of material selectivity on InP and InGaAsP. Two etching systems, $C_3H_8O_3:HCl:HClO_4$ and $H_2O:H_2SO_4:H_2O_2$, are investigated in detail. In terms of the etching-rate ratio, these compositions can be characterized by 10^{-3} and 50, respectively. The temperature dependence can be described by an activation energy of about 0.5 eV. This value, along with the insensitivity on stirring conditions and electron concentration of the etched crystals, is indicative of reaction-rate limitation. The selective property of the etchants was tested by producing a double-mesa-structure from heteroepitaxial layers. The test showed, that the etching systems described can be successfully

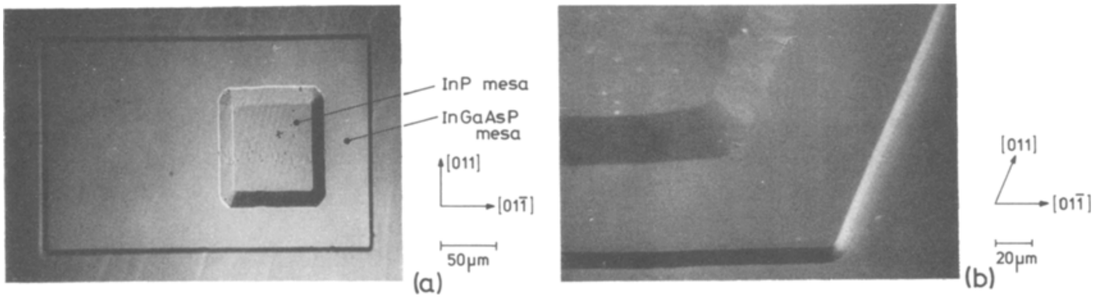

Figure 9 Double-mesa-structure on an InP/InGaAsP/InP layer sequence. First etching step: 2 min 15 sec in glycerine: $HCl:HClO_4 = 1:2:2$, second step: 5 min in $H_2O:H_2SO_4:H_2O_2 = 1:3:1$ all at 20° C. (a) Interference-contrast microphotograph. (b) Enlarged SEM photograph of the mesa ramps; InP-mesa height: 5.5 µm; InGaAsP-mesa height 3.1 µm.

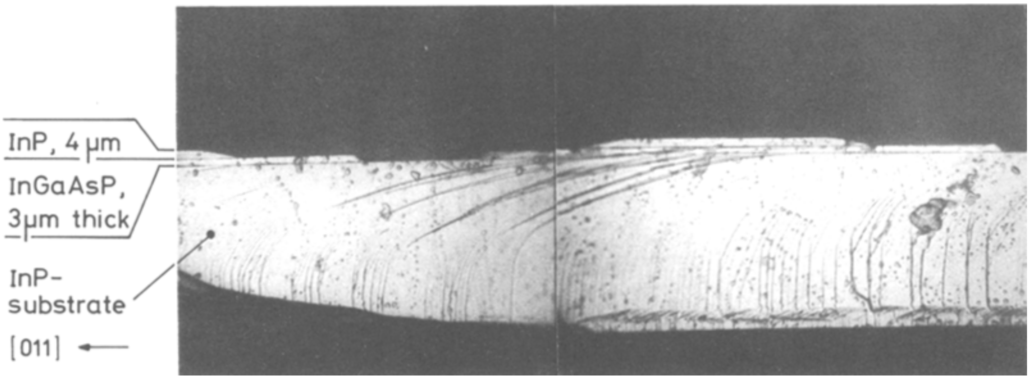

Figure 10 Cleavage plane of a mesa produced by the same procedure as that of Fig. 9.

applied to device fabrication by using standard photolithographic techniques.

Acknowledgements

These investigations were financially supported by the "Deutsche Forschungsgemeinschaft". The authors gratefully acknowledge a clarifying discussion with Dr B. Schwartz, Bell Telephone Laboratories, and the skilfull technical assistance by U. Heydecke in the epitaxial growth.

References

1. M. S. ABRAHAMS and C. J. BUIOCCHI, *J. Appl. Phys.* **36** (1965) 2855.
2. A. HUBER and N. T. LINH, *J. Crystal Growth* **29** (1975) 80.
3. F. A. THIEL and R. L. BARNS, *J. Electrochem. Soc.* **126** (1979) 1272.
4. T. KOTANI, S. KOMIYA, S. NAKAI and Y. YAMAOKA, *ibid.* **127** (1980) 2273.
5. G. T. BROWN, B. COCKAYNE and W. R. MacEWAN, *J. Mater. Sci.* **15** (1980) 2539.
6. Y. NISHITANI and T. KOTANI, *J. Electrochem. Soc.* **126** (1979) 2269.
7. T. KAMBAYASHI, C. KITAHARA and K. IGA, *Japan. J. Appl. Phys.* **19** (1980) 79.
8. S. ADACHI and H. KAWAGUCHI, *J. Electrochem. Soc.* **128** (1981) 1343.
9. S. B. PHATAK and G. KELNER, *ibid.* **126** (1979) 287.
10. D. FRITZSCHE, E. KUPHAL and R. AULBACH, *Electronics Lett.* **17** (1981) 178.
11. P. D. GREENE, *Solid-State Electronics* **19** (1976) 815.
12. R. P. TIJBURG and T. VAN DONGEN, *J. Electrochem. Soc.* **123** (1976) 687.
13. J. J. LePORE, *J. Appl. Phys.* **51** (1980) 6441.
14. W. KOWALSKY, A. SCHLACHETZKI and F. FIEDLER, *Phys. Stat. Sol. (a)* **68** (1981) 153.
15. W. KERN, *RCA Rev.* **39** (1978) 278.
16. B. TUCK and A. J. BAKER, *J. Mater. Sci.* **8** (1973) 1559.
17. K. AKITA, T. KUSUNOKI, S. KOMIYA and T. KOTANI, *J. Crystal Growth* **46** (1979) 783.
18. S. IIDA and K. ITO, *J. Electrochem. Soc.* **118** (1971) 768.
19. J. J. HSIEH and C. C. SHEN, *Appl. Phys. Lett.* **30** (1977) 429.

Received 29 January
and accepted 1 March 1982